World Journal of Engineering Research
Print ISSN: 2959-9865
Online ISSN: 2959-9873
DOI: https://doi.org/10.61784/wjer3141

MIXED-INTEGER LINEAR PROGRAMMING SCHEDULING MODEL FOR MICROGRID DAY-AHEAD POWER PROCUREMENT BASED ON QUANTILE PREDICTION

ChangWei Song
College of Sciences, Shihezi University, Shihezi 832000, China.

Abstract: Targeting the day-ahead dispatching scenario of microgrids featured by pronounced uncertainties in load and photovoltaic generation, in which power deficits will incur emergency electricity acquisition with heavy penalties, this paper develops a mixed-integer linear programming dispatching model grounded on quantile forecasting of historical net load. A rolling historical window is utilized to implement quantile estimation for net-load sequences, and a 7-day retrospective window paired with the 0.8 quantile is finalized as the forecasting setup after parameter tuning with January datasets. Binary decision variables are deployed to impose the mutual-exclusive restriction on battery charging and discharging behaviors. Daily pre-arranged electricity-acquisition and energy-storage operational schemes are computed at midnight, with intra-day responsive adjustment performed in accordance with practical source-load measurements. Closed-loop emulation outcomes spanning 334 days from February to December 2025 demonstrate that the aggregate electricity-acquisition expense across the entire horizon hits 16 034 311.14 CNY. Emergency electricity procurement takes place on 186 days, with the corresponding emergency energy volume amounting to 177 712.73 kWh. The devised model yields viable day-ahead electricity-acquisition tactics under partial source-load information and offers references for economical dispatching of community-scale microgrids furnished with energy-storage facilities.
Keywords: Microgrid; Day-ahead power procurement; Quantile prediction; Mixed-integer linear programming; Energy-storage scheduling

1 INTRODUCTION

The wide-scale integration of photovoltaic units brings prominent forecast uncertainties for community-scale grid-connected microgrids, which may cause severe power deficits and trigger high-cost emergency power-purchase penalties in practical day-ahead dispatching [1-2]. Energy-storage devices serve as critical flexible resources to offset source-load fluctuations and mitigate economic losses induced by prediction deviations [3-4]. Mixed-integer linear programming (MILP) provides a feasible modeling paradigm to describe physical restrictions such as the mutual exclusiveness of battery charging and discharging [5-6]. Nevertheless, many deterministic MILP dispatch models rely on perfect point forecasts and lack effective risk-resistant prediction modules oriented to practical penalty scenarios. Unreliable forecast inputs will directly degrade the practicability of optimized scheduling solutions in real-world microgrid operation. Reasonable prediction configuration is therefore the prerequisite to balance operational risk and procurement expenditure. Excessively conservative parameter settings will also raise baseline procurement costs and reduce overall economic returns.

Numerous existing studies have explored microgrid day-ahead optimization under renewable-energy uncertainties [7-8]. Probabilistic forecasting approaches including quantile estimation have been adopted to reserve safety margins for power scheduling, yet plenty of relevant works seldom calibrate sliding-window parameters on real historical datasets [9]. Few publications conduct long-term closed-loop emulation spanning hundreds of days to quantify the overall economic performance of quantile-driven MILP dispatching schemes under emergency-penalty mechanisms [10]. There still exists research gap for implementable frameworks combining empirical quantile prediction, storage physical constraints and full-period simulation assessment. Most existing works merely carry out short-term case tests rather than multi-month rolling validation under real penalty rules. Such simplified evaluation may overestimate the actual economic benefits of proposed dispatching tactics. Hence, sufficient long-run simulation tests are indispensable for verifying model reliability.

Targeting the above-mentioned research gaps, this work establishes a MILP day-ahead dispatching model for microgrid power procurement based on historical net-load quantile forecasting. Sliding-window parameters are calibrated using real-world January datasets, and binary variables are deployed to enforce charging-discharging mutual-exclusive constraints. Day-ahead decision-making is performed at midnight, and intra-day feedback adjustment together with emergency power-purchase settlement is executed for long-term closed-loop simulation. Numerical outcomes verify the economic practicability of the presented strategy under incomplete source-load information.

2 METHODOLOGY

2.1 Data Preprocessing

© By the Author(s) 2026, under the CC BY-NC-ND license (http://creativecommons.org/licenses/by-nc-nd/4.0).

This paper provides the electricity prices for 144 time intervals and the actual community load and photovoltaic power generation data for the whole year of 2025, respectively. In this subsection, the two datasets are aligned by date and time stamp to form two numerical matrices of size 365 × 144. After inspection, the original dataset contains no duplicate dates, the time sequence is continuous and complete, and no missing values exist in load and photovoltaic records.

The timestamp of each record is regarded as the end of the corresponding 10-min interval. The label 0:10 corresponds to the interval 00:00—00:10, and 0:00+1 represents 24:00 of the same day. The load power and actual photovoltaic power within the corresponding interval are denoted as $P_{d,t}^{L}$ and $P_{d,t}^{PV,a}$, respectively. Power values are converted into electric energy for each interval:

$$L_{d,t} = P_{d,t}^{L}\Delta t, V_{d,t}^{a} = P_{d,t}^{PV,a}\Delta t \tag{1}$$

Furthermore, the actual net load is defined as the difference between community load energy and photovoltaic energy:

$$R_{d,t} = L_{d,t} - V_{d,t}^{a} \tag{2}$$

where $R_{d,t} < 0$ indicates that photovoltaic energy exceeds the load in this interval, producing surplus photovoltaic power. This surplus energy can be used for subsequent energy storage charging. Negative values are retained in subsequent calculations instead of being truncated to zero.

2.2 Model Establishment

A two-stage strategy from day-ahead forecasting to intra-day feedback is adopted in this subsection. At 00:00 every day, historical data are first used to forecast the net load of all intervals on the target day. The forecast results are taken as model inputs to determine the planned electricity purchase quantity and energy storage scheduling scheme for the whole day. During actual operation, the charging and discharging of energy storage are adjusted in real time according to the actual load and photovoltaic output, and emergency power purchase is activated to fill the supply-demand gap.

For each date d and each time interval t, the α-quantile of the net load at the same time interval of the nearest K historical days is calculated as the net load forecast for this interval:

$$\hat{R}_{d,t} = Q_{\alpha}\left(\{R_{j,t}: \max(1, d-K) \le j < d\}\right) \tag{3}$$

where K denotes the length of the historical data window and α is the quantile level. When the available historical samples are fewer than K, all existing historical samples are adopted, and the default linear interpolation method of NumPy is used for quantile calculation.

To determine a reasonable α, the single-interval approximation without energy storage is considered first. Let the planned purchased power be $g \ge 0$, the actual net load be a random variable R, and $(x)^{+} = \max(x, 0)$ denote the positive part. If R > g, the planned purchased power is less than the actual demand and emergency power purchase is required. If $R \le g$, the purchased power already leads to extra procurement cost. Thus, the expected cost is formulated as:

$$J(g) = p_t g + 5p_t \mathbb{E}[(R-g)^{+}] \tag{4}$$

Under continuous distribution assumptions, when the objective function reaches its optimum inside the domain, the marginal cost brought by adding one unit of purchased power balances the reduction of expected emergency procurement cost:

$$J'(g) = p_t - 5p_t Pr(R > g) = 0 \Longrightarrow Pr(R \le g) = 0.8 \tag{5}$$

Based on the above analysis, $\alpha = 0.8$ is selected to reduce the probability of emergency power purchase while controlling procurement expenditure.

Besides the quantile level α, the historical window length K also affects forecasting results. A too-short historical window makes forecasts more sensitive to recent data and vulnerable to short-term fluctuations. A too-long window can incorporate more historical information but weakens the reflection of recent characteristics. Therefore, candidate window lengths of 7 days, 14 days and 28 days are tested. Simulations are carried out from January 15 to January 31 following the sequence of "forecasting — day-ahead scheduling — real-time adjustment". The optimal window is selected by minimizing the sum of planned procurement cost and emergency procurement cost:

$$K^{*} = \arg \min_{K \in \{7,14,28\}} \sum_{d=15}^{31} F_d(K) \tag{6}$$

Table 1 shows the calibrated cost of the three candidate windows:

Table 1 Calibration Cost of Historical Windows

Historical window / day	Cost from Jan.15 to Jan.31 / CNY
7	1024296.0245
14	1033387.2171
28	1047538.0979

The 7-day window achieves the lowest calibration cost, so $K = 7$ is adopted. This parameter is finalized at 00:00 on February 1. After that, the actual results from February to December are used to update the initial state of charge of energy storage.

After the forecast parameters are determined, the known net load in the model of Problem is replaced by the forecast value in Eq. (3). Subject to the same constraint set as Problem, the planned purchased power of the subsequent 144 intervals can be solved at 00:00 every day with the current stored energy as the initial state:

$$\begin{aligned}
\min \quad & F_d^p = \sum_{t=1}^{N} p_t G_{d,t} \\
\text{s.t.} \quad & G_{d,t} + D_{d,t}^p - C_{d,t}^p - S_{d,t}^p = \hat{R}_{d,t}, \\
& E_{d,t}^p = E_{d,t-1}^p + \eta_c C_{d,t}^p - \frac{D_{d,t}^p}{\eta_d}, \\
& E_{\min} \le E_{d,t}^p \le E_{\max}, \\
& 0 \le C_{d,t}^p \le P_{\max} \Delta t z_{d,t}^p, \\
& 0 \le D_{d,t}^p \le P_{\max} \Delta t \left(1 - z_{d,t}^p\right), \\
& G_{d,t}, S_{d,t}^p \ge 0, z_{d,t}^p \in \{0,1\}, \\
& E_{d,0}^p = E_{d,0}, E_{d,N}^p = 6000.
\end{aligned} \tag{7}$$

$S_{d,t}^p$ represents unused surplus energy under forecast conditions to avoid direct truncation of negative net load to zero. Since each scheduling interval lasts $\frac{1}{6}$h and the maximum charging/discharging power of energy storage is 5000 kW, the maximum charge and discharge energy in each interval is equal to 833.33 kWh.

The value 6000 kWh in Eq. (7) is the scheduled target stored energy at the end of each day. Setting this target prevents excessive consumption of energy storage which may lead to excessively low purchased power, and guarantees stable iteration of the model. This model contains 865 variables and 144 binary state variables per day. The HiGHS solver is adopted to obtain the integer feasible solution with minimum planned cost.

3 RESULTS

3.1 Model Solution

The planned $G_{d,t}$ remains fixed during the intra-day stage, and feedback adjustment is performed according to real-time photovoltaic and load data. The energy storage deviation without considering storage regulation is calculated first:

$$b_{d,t} = G_{d,t} + V_{d,t}^a - L_{d,t} \tag{8}$$

When $b_{d,t} \ge 0$, the supply satisfies load demand and surplus energy exists. The surplus energy is preferentially used to charge energy storage. The actual charging energy satisfies:

$$C_{d,t} = \min\left\{b_{d,t}, P_{\max}\Delta t, \frac{E_{\max} - E_{d,t-1}}{\eta_c}\right\}, D_{d,t} = H_{d,t} = 0 \tag{9}$$

If surplus energy still exists after charging, further distinction is made between unused planned power and abandoned photovoltaic power. Following the photovoltaic accounting rule, the unused portion within planned purchased power is defined as unused planned volume. Energy exceeding planned purchased power and unable to be absorbed by storage is defined as abandoned photovoltaic power:

$$U_{d,t} = \min\left\{G_{d,t}, b_{d,t} - C_{d,t}\right\}, W_{d,t} = b_{d,t} - C_{d,t} - U_{d,t} \tag{10}$$

When $b_{d,t} < 0$, the supply fails to meet load demand. Energy storage is discharged to fill the supply gap, and emergency power purchase is required for the uncompensated part:

$$D_{d,t} = \min\left\{-b_{d,t}, P_{\max}\Delta t, \eta_d\left(E_{d,t-1} - E_{\min}\right)\right\}, H_{d,t} = -b_{d,t} - D_{d,t}, C_{d,t} = U_{d,t} = W_{d,t} = 0 \tag{11}$$

Energy balance must hold for both surplus and shortage scenarios:

$$G_{d,t} + H_{d,t} + V_{d,t}^a - U_{d,t} - W_{d,t} + D_{d,t} = L_{d,t} + C_{d,t} \tag{12}$$

Stored energy is updated following the same efficiency relation. After operation, the stored energy is no longer forced to recover to 6000 kWh, and it serves as the initial stored energy for the next day:

$$E_{d,t} = E_{d,t-1} + \eta_c C_{d,t} - \frac{D_{d,t}}{\eta_d}, E_{d+1,0} = E_{d,N} \tag{13}$$

During operation, the cost of confirmed planned purchased power is calculated at the normal electricity price of the corresponding interval. Charges are still payable for unused planned purchased power, while emergency power purchase is settled at five times the normal price. Therefore, the actual total procurement cost on day d is:

$$F_d = \sum_{t=1}^{N} p_t G_{d,t} + \sum_{t=1}^{N} 5 p_t H_{d,t}, F = \sum_{d=32}^{365} F_d \tag{14}$$

A complete calculation workflow from forecasting to final settlement is formed based on the above modeling: net load forecasting is implemented using historical data; the all-day scheduling plan is formulated; energy storage is adjusted in real time during operation, and emergency procurement cost is computed. Daily planned purchased power, actual charge-discharge energy and emergency procurement results from February to December can be obtained by iterative calculation according to Eqs. (3), (7) and (5-8)—(14). The aggregated full-period cost and energy statistics are listed in Table 2. The total daily purchased energy equals the sum of planned purchased energy and emergency purchased energy, and the daily procurement cost includes both planned and emergency charges.

Table 2 Aggregated Full-Period Cost and Energy Statistics

Item	Result	Unit
Planned procurement cost	14928946.1863	CNY
Emergency procurement cost	1105364.9549	CNY

Item	Result	Unit
Total procurement cost	16034311.1412	CNY
Planned purchased energy	23929821.7380	kWh
Emergency purchased energy	177712.7311	kWh
Unused planned energy	3031809.5490	kWh
Days with emergency procurement	186	Day

As shown in Table 2, the total procurement cost reaches 16034311.1412 CNY, including 14928946.1863 CNY for planned purchase and 1105364.9549 CNY for emergency purchase. Emergency procurement accounts for approximately 6.89% of the total procurement cost.

According to the requirements, the procurement and energy storage results on two specified dates (June 21 and December 21) are extracted and summarized in Tables 3 to 6. Consecutive emergency procurement intervals are merged and listed in Table 7. Tables aggregate results over 4-hour intervals. Thus, charging and discharging energy may coexist within one aggregated interval, which correspond to different 10-min sub-intervals and do not imply simultaneous charging and discharging of the energy storage device.

Table 3 Purchased Energy in Specified Intervals, Daily Purchased Energy and Cost on Jun.21

Time interval	Purchased energy / kWh	Time interval	Purchased energy / kWh	Time interval	Purchased energy / kWh
10:00—10:10	0.0000	12:00—12:10	728.2969	14:00—14:10	0.0000
16:00—16:10	631.3660	18:00—18:10	690.1770	20:00—20:10	50.3672
Whole day	72972.2757	Whole-day cost	46188.6732		

Table 4 Charging/Discharging Energy and Initial/Final Stored Energy of Energy Storage on Jun.21 (kWh)

Time interval	Charging energy	Discharging energy	Time interval	Charging energy	Discharging energy
0:00—4:00	0.0000	0.0000	4:00—8:00	1226.3636	1297.7091
8:00—12:00	375.7463	0.0000	12:00—16:00	0.0000	0.0000
16:00—20:00	0.0000	3819.3380	20:00—24:00	6868.9918	1744.5453
Initial stored energy (00:00)	10800.0000	Final stored energy (24:00)		10800.0000	

Table 5 Purchased Energy in Specified Intervals, Daily Purchased Energy and Cost on Dec.21

Time interval	Purchased energy / kWh	Time interval	Purchased energy / kWh	Time interval	Purchased energy / kWh
10:00—10:10	0.0000	12:00—12:10	942.6802	14:00—14:10	0.0000
16:00—16:10	826.6481	18:00—18:10	719.4123	20:00—20:10	0.0000
Whole day	89751.6343	Whole-day cost	58848.2932		

Table 6 Charging/Discharging Energy and Initial/Final Stored Energy of Energy Storage on Dec.21 (kWh)

Time interval	Charging energy	Discharging energy	Time interval	Charging energy	Discharging energy
0:00—4:00	117.6082	213.0872	4:00—8:00	1019.7473	1541.3953
8:00—12:00	5492.1597	7500.6131	12:00—16:00	7638.1271	2301.6946
16:00—20:00	219.664	5882.4702	20:00—24:00	5531.8473	2785.6751
Initial stored energy (00:00)	10800.0000	Final stored energy (24:00)		6167.1598	

Table 7 Emergency Purchased Energy on Specified Dates (kWh)

Mar.20 Interval	Energy	Jun.21 Interval	Energy	Sep.23 Interval	Energy	Dec.21 Interval	Energy
20:30—20:40	181.6270	None	0.0000	09:10—09:50	141.7842	20:30—20:40	67.2032
21:20—21:40	17.1955			20:20—20:40	1393.7250		
				20:50—21:10	65.3582		

3.2 Result Analysis

To further evaluate the practical operation performance, the results are analyzed from three perspectives: annual cost composition, energy storage state on specified dates and constraint satisfaction. First, Figure 1 presents the monthly statistics of planned procurement cost, emergency procurement cost and total procurement cost from February to December.

As illustrated in Figure 1, the procurement cost exhibits obvious seasonal variation. Taking September 23 as an example, Figure 2 plots the evolution of actual stored energy over time.

It can be observed from Figure 2 that the stored energy approaches or hits the upper and lower bounds successively, which reflects the combined effect of supply-demand variation and equipment capacity limits.

To verify the correctness of results, constraint checking is performed for all 48096 time intervals, including actual supply-demand balance, stored energy recurrence relation, upper/lower bounds, charge-discharge power limits, charge-discharge mutual exclusiveness, and continuity of stored energy between adjacent days. All checks pass. The maximum constraint residual is 4.54×10^{-12}, smaller than the preset tolerance of 10^{-6}, which demonstrates good numerical stability of the model. In addition, the maximum relative integer gap of the 334 day-ahead models is

approximately 3.05×10^{-16}, indicating that optimal solutions are obtained for all day-ahead optimization problems under given forecast data and parameters.

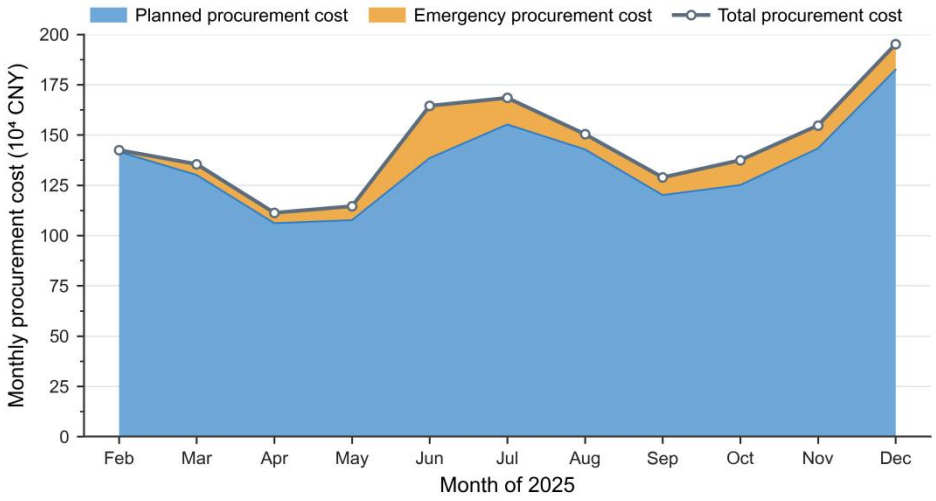


Figure 1 Monthly Composition of Procurement Cost

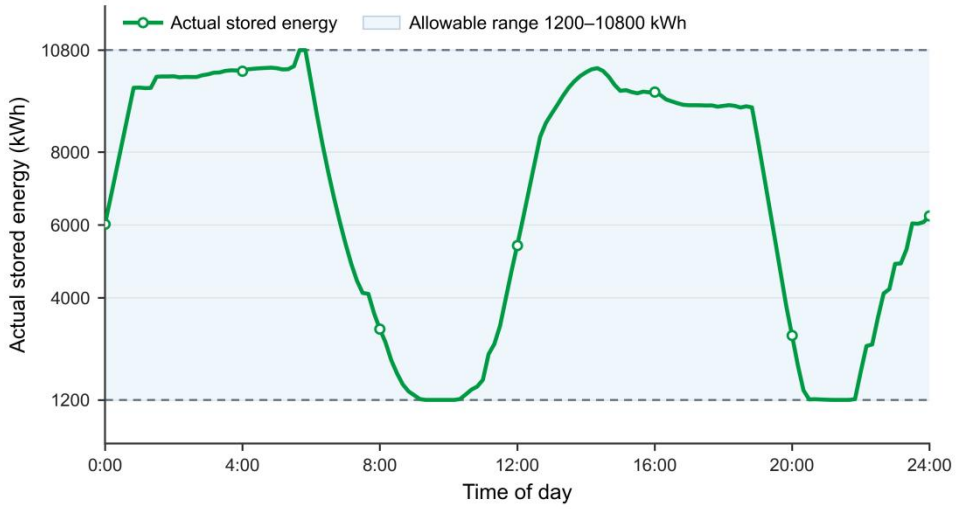


Figure 2 Actual Stored Energy on September 23

4 CONCLUSIONS

This work develops a mixed-integer linear programming dispatching model for community microgrid day-ahead power procurement based on historical net-load quantile forecasting. Through parameter calibration with early-stage real-world data, a 7-day sliding window and 0.8 quantile are determined for probabilistic prediction. Binary variables are adopted to impose mutual-exclusive constraints on battery charging and discharging behaviors. Long-term closed-loop emulation covering 334-day real-world operation verifies the economic performance of the proposed framework under emergency-purchase penalty rules. The whole modeling workflow can be solved by mature open-source MILP solvers, which facilitates migration to practical community microgrid operation platforms and possesses favorable engineering practicability for day-ahead procurement decision-making.

Nevertheless, this research still has several inherent limitations. The quantile-based forecasting strategy heavily relies on historical source-load records and may fail to handle unprecedented extreme meteorological scenarios beyond existing datasets. For future research, more advanced probabilistic forecasting techniques can be introduced to improve prediction adaptability under out-of-sample conditions. Time-varying battery degradation parameters can be incorporated into the optimization formulation. Furthermore, extended simulation research under time-varying electricity-price mechanisms can be carried out to broaden the application scope of the presented dispatching approach.

COMPETING INTERESTS

The authors have no relevant financial or non-financial interests to disclose.

REFERENCES

[1] Babatunde O, Fasesin K, Dosa A, et al. Multi-Stage Stochastic MILP Framework for Renewable Microgrid Dispatch Under High Renewable Penetration: Optimizing Variability and Uncertainty Management. Applied Sciences, 2025, 15(19): 10303.
[2] Akarne Y, Essadki A, Nasser T, et al. Enhanced smart microgrid scheduling: An empirical study on simultaneous energy supply and demand optimization using binary sparrow search algorithm. Results in Engineering, 2025, 27: 106811.
[3] Fritz M J, Riebesel L, Xhonneux A, et al. MASSIVE: A scalable framework for agent-based scheduling of micro-grids using market mechanisms. Energy Informatics, 2025, 8(1): 101.
[4] Mas'ud A A, Seidu I, Salisu S, et al. Wind energy assessment and hybrid micro-grid optimization for selected regions of Saudi Arabia. Scientific Reports, 2025, 15(1): 1376.
[5] Güven F A, Hassan H M, Kamel S. Optimization of a hybrid microgrid for a small hotel using renewable energy and EV charging with a quadratic interpolation beluga whale algorithm. Neural Computing and Applications, 2024, 37(5): 1-36.
[6] Zeng Q G, Qin Z, Lu D K, et al. CMOPEO-OP: Constrained multi-objective population extremal optimization-based optimal planning of standalone microgrids. Swarm and Evolutionary Computation, 2025, 92: 101787.
[7] Khan A M, Rehman T, Kim M H. Optimal operation of hydrogen-based multi-energy microgrid integrating water network and transportation sector. International Journal of Hydrogen Energy, 2025, 97: 501-515.
[8] Sun H, Duan Z, Yang A. Microgrid Optimization Strategy for Charging and Swapping Power Stations with New Energy Based on Multi-Agent Reinforcement Learning. Sustainability, 2024, 16(23): 10663.
[9] Jayaraj S, Abraham P M, T.P. A I, et al. Efficient microgrid scheduling via actor-critic reinforcement learning with minimal state representation and well-defined reward design. Energy Reports, 2025, 14: 3591-3604.
[10] Nouri F, Dahraie V M, Shariatinasab R, et al. A decision-making framework for multi-microgrids scheduling considering joint P2P energy and reserve trading floor. Sustainable Energy, Grids and Networks, 2025, 42: 101685.